Experimental Neurology 248 (2013) 530–540

Contents lists available at ScienceDirect

Experimental Neurology

journal homepage: www.elsevier.com/locate/yexnr

Functional characterization of ClC-1 mutations from patients affected by recessive myotonia congenita presenting with different clinical phenotypes

Jean-François Desaphy [a,*], Gianluca Gramegna [a], Concetta Altamura [a], Maria Maddalena Dinardo [a], Paola Imbrici [a], Alfred L. George Jr. [b], Anna Modoni [c], Mauro LoMonaco [c], Diana Conte Camerino [a]

[a] Section of Pharmacology, Department of Pharmacy & Drug Sciences, University of Bari-Aldo Moro, Bari, Italy
[b] Division of Genetic Medicine, Vanderbilt University, Nashville, TN, USA
[c] Department of Neurosciences, Catholic University, Rome, Italy

ARTICLE INFO

Article history:
Received 11 June 2013
Revised 18 July 2013
Accepted 25 July 2013
Available online 8 August 2013

Keywords:
Acetazolamide
Chloride channel mutation
ClC-1 chloride channel
Genotype–phenotype relationship
Myotonia congenita
Non-dystrophic myotonia
Patch-clamp
Transitory weakness

ABSTRACT

Myotonia congenita (MC) is caused by loss-of-function mutations of the muscle ClC-1 chloride channel. Clinical manifestations include the variable association of myotonia and transitory weakness. We recently described a cohort of recessive MC patients showing, at a low rate repetitive nerves stimulation protocol, different values of compound muscle action potential (CMAP) transitory depression, which is considered the neurophysiologic counterpart of transitory weakness. From among this cohort, we studied the chloride currents generated by G190S (associated with pronounced transitory depression), F167L (little or no transitory depression), and A531V (variable transitory depression) hClC-1 mutants in transfected HEK293 cells using patch-clamp. While F167L had no effect on chloride currents, G190S dramatically shifts the voltage dependence of channel activation and A531V reduces channel expression. Such variability in molecular mechanisms observed in the hClC-1 mutants may help to explain the different clinical and neurophysiologic manifestations of each ClCN1 mutation. In addition we examined five different mutations found in compound heterozygosis with F167L, including the novel P558S, and we identified additional molecular defects. Finally, the G190S mutation appeared to impair acetazolamide effects on chloride currents in vitro.

Introduction

Recessive (Becker's disease) and dominant (Thomsen's disease) myotonia congenita are caused by mutations in the *CLCN1* gene encoding the voltage-dependent chloride ClC-1 channel quite exclusively expressed in the sarcolemma (George et al., 1993; Koch et al., 1992). Mutations impair ion channel function and/or expression, and are predicted to reduce sarcolemmal chloride conductance that normally stabilizes muscle fiber membrane potential. A chloride conductance reduced by more than 50% predisposes to membrane hyper-excitability characterized by spontaneous action potential runs or abnormal after-discharges that impede muscle relaxation upon cessation of nerve input. Functional ClC-1 channels are composed of two identical subunits, each forming an independent chloride ion-conducting pore (Saviane et al., 1999). A dominant ClC-1 mutant is thus expected to exert a dominant-negative effect on the associated wild-type (WT) subunit in order to reduce the chloride conductance enough to evoke clinical myotonia. On the other hand, a recessive mutation likely affects only the encoded subunit, and both alleles must be mutated to cause the disease.

Myotonia congenita is clinically characterized by two contrasting phenomena: the abnormal membrane excitation leading to myotonia and the muscle inexcitability manifesting as transitory weakness (Trip et al., 2009). Interestingly, a significant clinical variability is usually observed in patients affected by either dominant or recessive forms of the disease and only a few studies have addressed the detailed genotype/phenotype relationship (Colding-Jorgensen, 2005). The functional characterization of ClC-1 channel mutations is however of great clinical relevance, because this should help to reveal the underlying mechanisms of each specific symptom and to define strategies to better address treatment in individual myotonic patients. For instance, we recently showed that patients suffering from sodium channel myotonia may obtain huge therapeutic improvements from such a pharmacogenetics strategy (Desaphy et al., 2004, 2013). Indeed, although the usefulness of mexiletine in sodium and chloride channel myotonias has been recently confirmed by a clinical trial (Statland

* Corresponding author at: Sezione di Farmacologia, Dipartimento di Farmacia-Scienze del Farmaco, via Orabona 4 — campus, 70125 Bari, Italy.
E-mail address: jfdesaphy@farmbiol.uniba.it (J.-F. Desaphy).

0014-4886
http://dx.doi.org/10.1016/j.expneurol.2013.07.018

et al., 2012), we have demonstrated that some sodium channel mutations are less responsive to mexiletine in vitro, and that patients carrying those mutations may greatly benefit from another drug, such as flecainide.

In a recent study, we described a cohort of patients affected by autosomal recessive MC (Modoni et al., 2011). We performed a low-rate repetitive nerve stimulation protocol to detect transitory depression of the compound action potential, which represents the neurophysiologic counterpart of transitory weakness (Aminoff et al., 1977). We observed that patients heterozygous for the G190S mutation presented with pronounced transitory depression and transitory weakness, whereas these features were very limited in patients carrying the F167L mutation. By contrast, patients heterozygous for the A531V mutation showed a remarkable variation in transitory depression. On the basis of these observations, the present study was undertaken to characterize the biophysical behavior of G190S, F167L, and A531V channel mutants expressed in HEK293 cells using the patch-clamp technique. Because chloride currents generated by F167L appeared quite similar to wild-type ones, we also studied the effects of five different mutations found in patients with compound heterozygosity for F167L and R105C, G284R, G355R, Y686X, or a newly discovered mutation (P558S). The experiments were performed using an intracellular solution containing low amount of chloride (4 mM), which is close to the physiological concentration in muscle fibers, or larger amount of chloride (134 mM), which allows to record huge chloride currents and to easily analyze deactivation kinetics. In addition, we report the effects of acetazolamide on wild-type and G190S chloride currents, because the drug has been shown to negatively shift the voltage-dependence of channel activation (Eguchi et al., 2006).

Material and methods

Site-directed mutagenesis and expression of WT and mutant hClC-1 channels

Mutations were introduced into the plasmid pRcCMV-hClC-1 containing the full-length wild-type (WT) hClC-1 cDNA using the QuickChange™ site-directed mutagenesis kit (Stratagene Cloning Systems). The complete coding region of the cDNA was sequenced to exclude polymerase errors. At least two independent mutant clones were tested for electrophysiological studies. Human embryonic kidney 293 (HEK293) cells were transiently transfected with a mixture of the hClC-1 (10 μg) and CD8 reporter plasmids (1 μg) using the calcium–phosphate precipitation method (Desaphy et al., 2001). Cells were examined between 36 and 80 h after transfection. Only cells decorated with anti-CD8 antibody-coated microbeads (Dynabeads M450, Invitrogen) were used for patch-clamp recordings.

Electrophysiology

Standard whole-cell patch-clamp recordings were performed at room temperature (~20 °C) using an Axopatch 200B amplifier (Axon Instruments). The composition of the extracellular solution was (in mM): 140 NaCl, 4 KCl, 2 $CaCl_2$, 1 $MgCl_2$ and 5 HEPES, and the pH was adjusted to 7.4 with NaOH. The high-chloride pipette solution contained (in mM): 130 CsCl, 2 $MgCl_2$, 5 EGTA and 10 HEPES, and the pH was adjusted to 7.4 with CsOH. In this condition, the equilibrium potential for chloride ions was about −2.8 mV and cells were clamped at the holding potential (hp) of 0 mV. In the low-chloride internal solution, cesium chloride was substituted by cesium glutamate. With this pipette solution, the equilibrium potential for chloride ions was about –92 mV and cells were clamped at the hp of –95 mV. Pipettes were pulled from borosilicate glass and had ~3 MΩ resistance, when filled with the above pipette solutions. For pharmacological experiments, acetazolamide (ACTZ, Sigma-Aldrich) was first dissolved in dimethylsulfoxide (DMSO) then in the external patch solution at the desired final concentration. The final DMSO concentration did not exceed 0.2% (vol/vol) and had no effect on HEK293 cell currents. The patched cell was continuously exposed to a stream of control or drug-supplemented bath solution flowing out from a plastic capillary.

Currents were low-pass filtered at 2 kHz and digitized with sampling rates of 50 kHz using the Digidata 1440A AD/DA converter (Axon Instr.). Patches with a series resistance voltage error greater than 5 mV and those with non-negligible leak current were discarded. Chloride currents were recorded ~5 min after achieving the whole cell configuration, to allow the pipette solution to equilibrate with the intracellular solution. Voltage-dependent channel activity was measured by applying specific voltage step pulses from the hp depending on the internal chloride concentration, as described in the Results section and shown in the figures. Voltage steps were applied every 3 s to allow complete recovery of current amplitude at the hp between two pulses. Data were analyzed off-line by using pClamp 10.3 (Axon Instruments) and SigmaPlot 8.02 (Systat Software GmbH) software. All data are presented as the mean ± SEM from N patches. The instantaneous and isochronal current–voltage relationships were drawn by measuring instantaneous and steady-state currents at the beginning (~1 ms) and end (~390 ms) of each voltage step. The voltage-dependence of channel activation was examined by plotting the apparent open probability (Po) as a function of membrane potential at the end of the test pulse. The Po was calculated from normalized instantaneous current amplitude measured at the start of the tail pulse at −105 mV. The relationship was fitted with a Boltzmann function,

$$Po(V) = Min + (1-Min)/\{1 + \exp[(V-V_{0.5})/S]\} \quad (1)$$

where Min is the minimal value of Po, $V_{0.5}$ is the half-maximal activation potential, and S is the slope factor. A double Boltzmann function was necessary to fit the activation curve of P558S mutant,

$$Po(V) = Min + A_1/\{1 + \exp[(V-V_1)/S_1]\} + A_2/\{1 + \exp[(V-V_2)/S_2]\}. \quad (2)$$

The time course of current deactivation was examined by fitting the decay of currents elicited in symmetrical chloride condition between −200 and −60 mV in 10-mV intervals with a sum of two exponentials and a time-independent component,

$$I(t) = A_{fast} \cdot \exp(t/\tau_{fast}) + A_{slow} \cdot \exp(t/\tau_{slow}) + C \quad (3)$$

where τ_{fast} and τ_{slow} are the time constants of the fast and slow components of current relaxation, and A_{fast}, A_{slow}, and C are the relative amplitudes of the fast, slow, and steady-state components of the current.

Results are reported as mean ± SEM from N cells, and statistical analysis was performed using Student's *t*-test, with $P < 0.05$ considered as significant.

Results

Clinical phenotype of myotonia congenita patients

The clinical phenotype of patients carrying all the mutations studied here except P558S was described previously (Modoni et al., 2011). Briefly, three unrelated patients were found to carry the G190S mutation in combination with 3 different mutations on the opposite allele. All three patients showed a pronounced transitory depression (>50%) upon neurophysiological examination using a 3-Hz repetitive nerve stimulation protocol. Three individuals from two families carrying the A531V mutation with compound heterozygosity for two different nonsense mutations displayed a remarkable variability of transitory depression upon successive examinations. Finally, eleven patients from 8 families had the F167L mutation in combination with 7 other mutations on the opposite allele. All these patients showed a limited transitory depression ranging from 0 to 23%. The seven compound

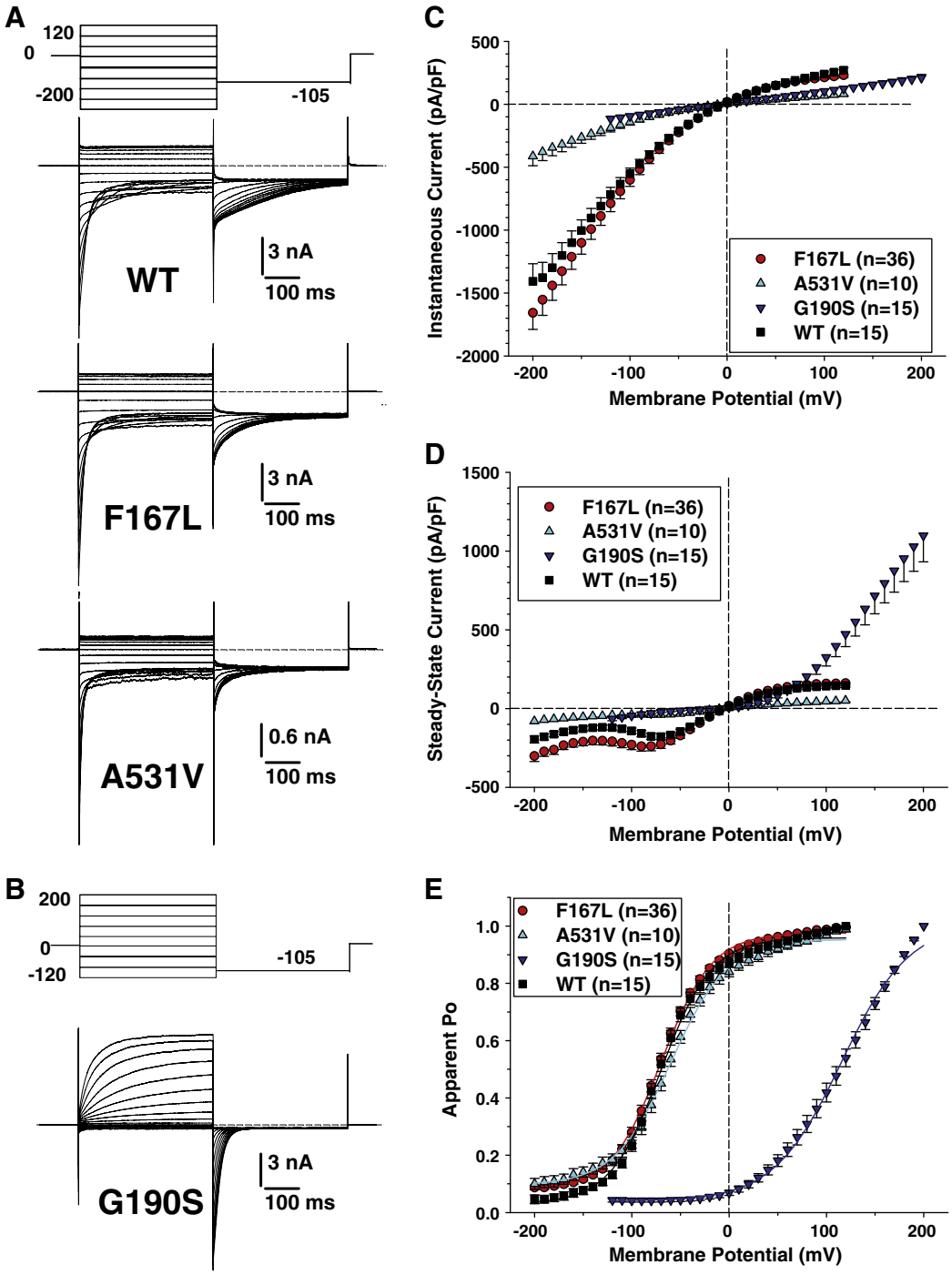

Fig. 1. Voltage-dependence of wild-type and F167L, A531V, and G190S myotonic hClC-1 channels in high intracellular chloride. A) Chloride currents were recorded in HEK293 cells transfected with wild-type, F167L, or A531V hClC-1 variants. Cells were held at 0 mV and 400 ms voltage pulses were applied from −200 to +120 mV in 10-mV intervals every 3 s. For clarity only current traces obtained every 20 mV are shown. Chloride currents displayed similar kinetics, but A531V had reduced amplitude. B) Voltage pulses were applied from −120 to +200 mV to elicit chloride currents in HEK293 cells expressing G190S hClC-1 variant. C) The instantaneous currents were measured at the beginning of test voltage pulses, normalized with respect to cell capacitance (pA/pF), and reported as a function of voltage. Each point is the mean ± SEM from 10 to 36 cells. The relationships show strong inward rectification for WT, F167L, and A531V channels, although current density was greatly reduced for A531V. The relationship for G190S channels was linear. D) Steady-state currents were measured at the end of test voltage pulses and reported as mean current density ± SEM in function of voltage. The WT and F167L relationships were very similar, while A531V generated reduced current densities. The G190S relationship shows a strong outward rectification. E) The voltage dependence of activation was determined by plotting the apparent open probability (Po), calculated from tail currents measured at −105 mV, as a function of test voltage pulses. The relationships obtained from averaged data were fit with a Boltzmann equation, and fit parameters are reported in Table 1. The activation curves for WT, F167L, and A531V were superimposable, whereas G190S channels displayed a positively-shifted voltage dependence.

mutations associated with F167L include 2 intronic, 4 exonic, and 1 unknown mutation. In the present study, we performed the biophysical characterization of G190S, A531V, and F167L mutants together with the 4 exonic mutants associated with F167L (R105C, G284R, G355R, Y686X). We also included the biophysical examination of the new P558S mutation found in combination with F167L in an additional MC

patient. This new mutation was found in a sporadic case coming from Southern Italy. The patient showed a very severe phenotype, with generalized muscle hypertrophy, in particular of lower limbs, muscle stiffness, severe myotonia and transitory weakness.

Characterization of mutations associated with various levels of CMAP transient depression

Chloride currents were elicited in HEK293 cells transfected with the same amount of either wild-type, F167L, G190S, or A531V hClC-1 chloride channels, using a voltage protocol allowing the determination of I–V relationships as well as the voltage dependence of activation (apparent open probability). Results obtained using high intracellular chloride concentration (134 mM) are shown in Fig. 1. Regarding WT, F167L, and A531V mutants, cells were held at 0 mV, and voltage steps were applied between −200 mV and +120 mV in 10 mV intervals, each followed by a voltage step at −105 mV (Fig. 1A). Preliminary observations concerning G190S showing low chloride current amplitude and lack of plateau led us to explore a different voltage range; thus depolarizing steps were applied between −120 mV and +200 mV (Fig. 1B). Time between two depolarizing steps was long enough to maintain a constant current at the holding potential. For WT, F167L, and A531V channels, instantaneous currents were observed at each voltage steps, which decreased over time at negative voltages between −200 and about −60 mV (corresponding to channel deactivation) or remained stable over time between −50 and +120 mV. Current amplitudes saturated at voltages greater than +50 mV. In contrast, G190S channels produced very little currents at negative voltages, and slowly activating currents at positive voltages. These currents did not saturate at voltages up to +200 mV.

Instantaneous and steady-state current densities (pA/pF) were calculated in at least n = 10 cells for each channel variant to draw mean instantaneous and isochronal I–V relationships (Figs. 1C, D). For instantaneous currents, the inwardly-rectifying relationships were nearly superimposable for WT and F167L channels, whereas current densities were greatly reduced at each voltage for A531V and G190S channels. Again, for steady-state currents, the I–V curves for WT and F167L channels were superimposable, and currents flowing through A531V were greatly lower. In contrast, the I–V relationships of G190S channels showed a strong outward rectification; compared to WT, G190S current densities were greatly reduced at membrane voltages within the physiological range and increased only at very positive voltages.

Voltage dependence of channel activation was determined by plotting the apparent open probability (normalized instantaneous currents at −105 mV) versus the voltage of preceding pulses (Fig. 1E). The relationships for WT, F167L, and A531V channel variants were well fit with a Boltzmann equation (Eq. (1)) and calculated parameters are given in Table 1. No significant differences were found between the three channel types. For G190S, no current saturation was observed and the maximum current for normalization was arbitrarily taken at +200 mV to draw the relationship. The voltage dependence of G190S channels appeared significantly shifted toward positive potentials.

With a low intracellular chloride concentration (4 mM), chloride currents were elicited from the conditioning voltage at −95 mV by a series voltage steps between −150 and +150 mV (−145 and +215 mV for G190S) applied every 3 s in 10-mV intervals, followed by a step to −105 mV (Fig. 2). In these conditions, chloride current kinetics were similar between the four channel variants, with instantaneous currents that remained quite stable over time at the more negative voltages or followed by slowly activating currents at less negative or positive voltages. Again, current amplitude plateau was observed at the more positive voltages except for G190S. Moreover current densities for A531V and G190S mutants were smaller compared to WT and F167L channels in the entire voltage range (Figs. 2C, D). The voltage dependence of activation was similar for WT and F167L (Fig. 2E, Table 1). For A531V, the relationship was steeper and the half-maximum activation voltage was slightly but significantly shifted. For G190S, the relationship was greatly shifted toward positive potentials.

Table 1
Boltzmann parameters of activation relationships of different ClC-1 variants using various internal chloride concentrations.

Variant	$[Cl^-]i$ (mM)	N	$V_{0.5}$ (mV)	S	Min
WT	134	15	−69.2 ± 2.3	25.0 ± 1.2	0.04 ± 0.01
	44	10	−56.7 ± 2.1	27.5 ± 2.2	0.02 ± 0.01
	24	8	−47.1 ± 4.2	30.9 ± 2.3	0.01 ± 0.01
	4	8	−30.0 ± 5.0	34.6 ± 3.3	0.02 ± 0.01
F167L	134	36	−70.3 ± 2.4	24.8 ± 0.6	0.08 ± 0.01*
	44	5	−57.6 ± 6.1	24.9 ± 1.6	0.02 ± 0.01
	24	8	−45.5 ± 3.0	30.8 ± 2.1	0.01 ± 0.01
	4	7	−26.2 ± 4.0	27.1 ± 1.4	<0.01
A531V	134	10	−59.6 ± 2.8*	29.4 ± 2.0	0.09 ± 0.02
	4	9	−16.4 ± 3.1*	60.0 ± 3.2*	0.08 ± 0.02*
G190S	134	15	+114.5 ± 4.5*	32.9 ± 1.3*	0.04 ± 0.01
	4	9	+111.9 ± 11.6*	42.0 ± 2.0	0.02 ± 0.01
R105C	134	6	−73.9 ± 6.4	21.1 ± 1.4	0.11 ± 0.03*
	4	6	−39.8 ± 7.1	35.3 ± 2.2	<0.01
P558S	134	8	V_1 = −62.9 ± 2.2 V_2 = +100.5 ± 4.2	S_1 = 17.0 ± 0.8 S_2 = 32.9 ± 3.3	0.28 ± 0.02*
	4	24	n.d.	n.d.	n.d.

The internal chloride concentration was modified by substituting glutamate for chloride ions. The external chloride concentration was maintained constant at 150 mM. The activation relationships obtained in each cell were fit with a Boltzmann equation (Eq. (1)) or a double Boltzmann equation for P558S (Eq. (2)), and fit parameters are reported as the mean ± SEM from N cells. $V_{0.5}$ is the half-maximum activation voltage, S is the slope factor, and Min is the minimal open probability. n.d. not determined.* indicates significant difference (at least $P < 0.05$) versus WT at the same internal chloride concentration, as calculated with unpaired Student's *t* test. Statistical analysis was not performed for $V_{0.5}$ and S values of P558S mutant. The mean relationships obtained from N cells are shown in Figs. 1D, 2D, and 6C.

The lower current densities observed for A531V and G190S within the physiological range of membrane potentials likely account for the manifestation of clinical myotonia. In contrast, F167L mutant appeared very similar to WT, and we thus performed further analysis of this mutant. We repeated the same protocols using pipette solutions containing intermediate chloride concentrations, 24 and 44 mM, and found no difference between WT and F167L in current densities (not shown) or in voltage dependence of activation (Table 1). We also analyzed the kinetics of current deactivation as a function of voltage in high-chloride condition. Deactivating currents were fitted with a double exponential function including a residual current (Eq. (3)). No difference was found between WT and F167L in the two time constants and in the relative amplitude of the fast, slow, and non-deactivating components (Fig. 3).

Characterization of mutations associated with F167L in heterozygous carriers

We characterized the function of ClC-1 mutants associated with F167L mutation in heterozygous patients, carrying R105C, G284R, G355R, Y686X (Modoni et al., 2011), and the newly identified P558S mutation, on the second allele.

In cells transfected with G284R, G355R, or Y686X, linear currents of low amplitude most likely corresponding to leak currents were recorded independent of the internal chloride ion concentration (Fig. 4).

Using high or low chloride intracellular concentration, chloride currents flowing through R105C were very similar to WT currents (Fig. 5). Only current density at steady-state was slightly smaller for R105C compared to WT (Figs. 6A, B). The voltage dependences of activation of WT and R105C were superimposable (Fig. 6C). Deactivation kinetics of R105C currents were also very similar to those of WT channels (Fig. 3).

The cells transfected with P558S showed a singular alteration of chloride current gating. Using high intracellular chloride conditions, chloride

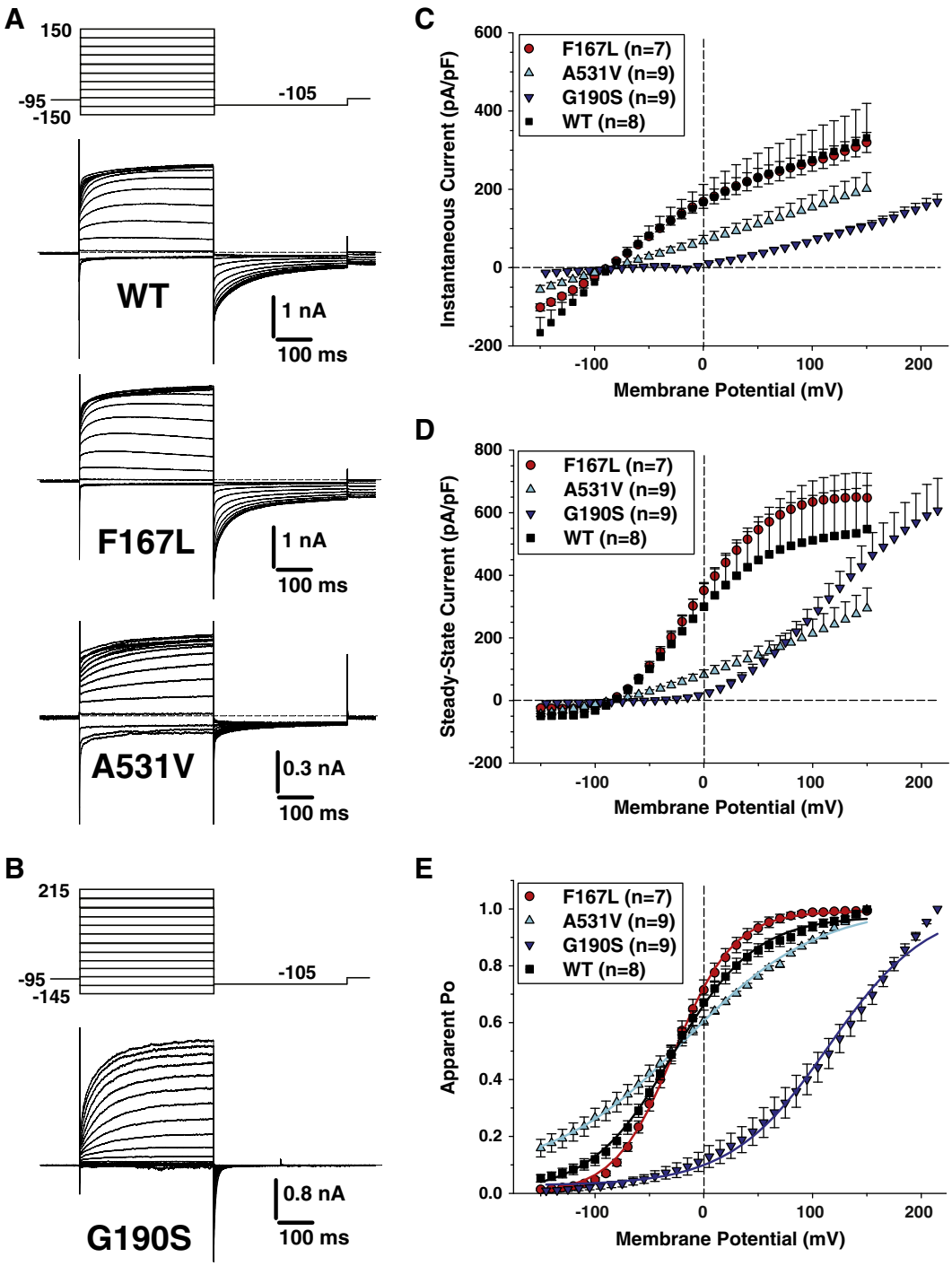

Fig. 2. Voltage-dependence of wild-type and F167L, A531V, and G190S myotonic hClC-1 channels in low intracellular chloride. A) Chloride currents were recorded in HEK293 cells transfected with wild-type, F167L, or A531V hClC-1 variants. Cells were held at −95 mV and 400 ms voltage pulses were applied from −150 to +150 mV in 10-mV intervals every 3 s. For clarity only current traces obtained every 20 mV are shown. Chloride currents displayed similar kinetics, but A531V had reduced amplitude. B) Voltage pulses were applied from −145 to +215 mV to elicit chloride currents in HEK293 cells expressing G190S hClC-1 variant. C) The instantaneous current density–voltage relationships were obtained as in Figs. 1C. D) The steady-state current density–voltage relationships were drawn as in Figs. 1D. E) The voltage dependence of activation, determined as in Fig. 1D, were fit with a Boltzmann function (Eq. (1)). Fit parameters are reported in Table 1. The activation voltage dependences of WT, F167L, and A531V show little variation, whereas G190S channels displayed a positively-shifted voltage dependence.

currents displayed a rapid deactivation followed by a slow activation at negative voltages (Fig. 5). At potentials positive to −100 mV, the kinetics of P558S currents were very similar to that of WT, but current densities were greatly reduced (Figs. 6A, B). In high-chloride condition, the apparent Po of P558S was best fit with a double Boltzmann function (Eq. (2)) and showed a significant residual Po at negative voltages with about 30% of channels remaining open between −200 and −100 mV (Fig. 6C, Table 1). In low chloride conditions, very small P558S currents were recorded, which did not saturate at positive voltages. Thus the activation curve was drawn by arbitrarily normalizing to currents measured at +150 mV. Because of lack of saturating currents, the fit of activation curve of P558S with a Boltzmann equation was not satisfactory;

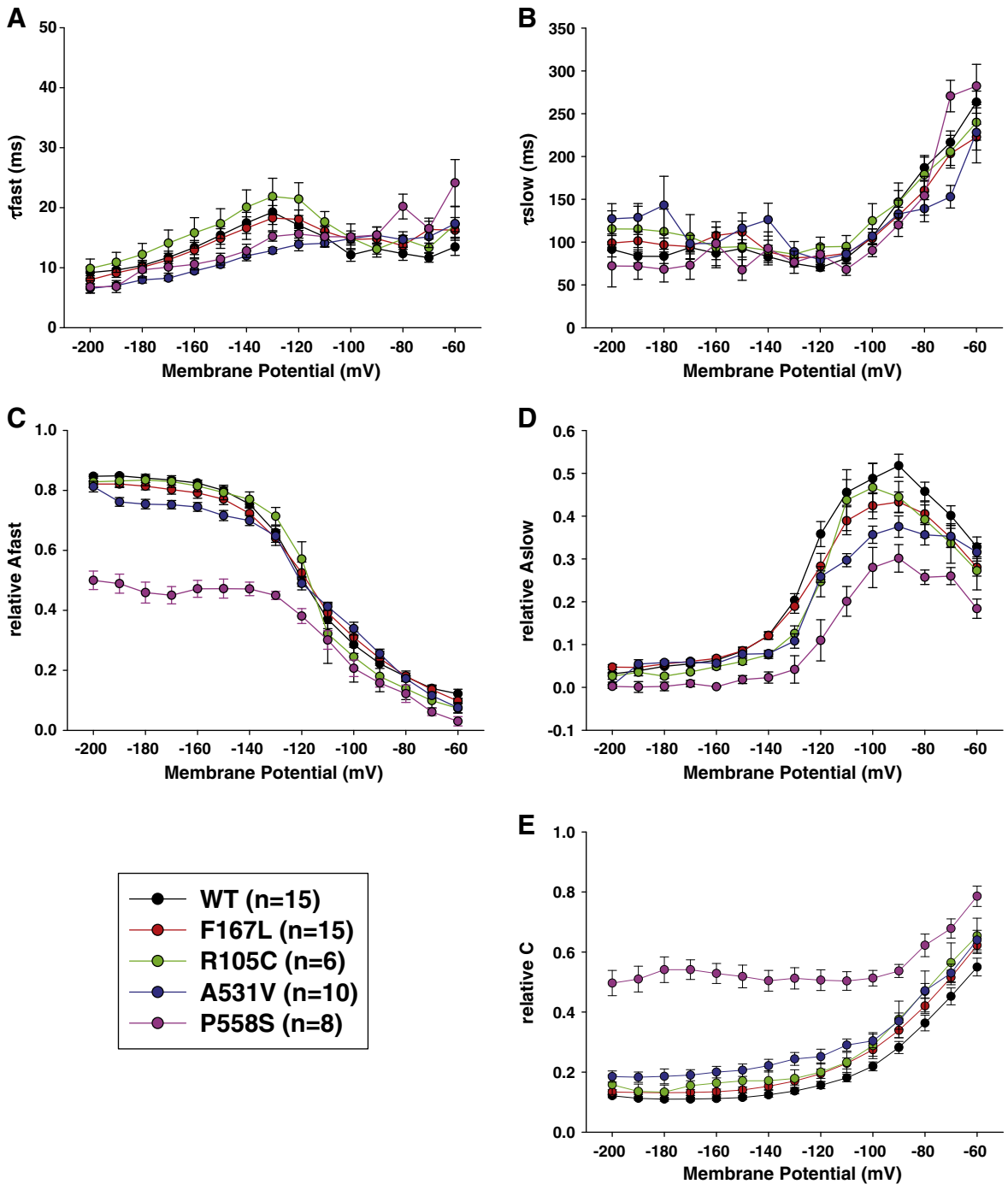

Fig. 3. Kinetics of deactivating currents for wild-type and F167L, R105C, and P558S myotonic hClC-1 channels in high intracellular chloride. The deactivating currents measured at the beginning of test voltage pulse between −200 and −60 mV were fit with a double exponential decay function (Eq. (3)). The fit parameters include a fast time constant (A, τ_{fast}, 10-ms range), a slow time constant (B, τ_{slow}, 100-ms range), and their respective contribution to total current (C: A_{fast}, and D: A_{slow}), plus the contribution of residual steady state current (E).

the estimated half-maximum activation voltage was approximately +25 mV. Analysis of deactivation kinetics indicates that the fast and slow time constants are similar to those found in WT (Fig. 3). However, compared to WT, the deactivation was incomplete at potentials more negative to −100 mV, with a greater steady state current.

Effects of acetazolamide on WT and G190S hClC-1 channels

Acetazolamide (ACTZ) is an inhibitor of carbonic anhydrase empirically used to treat myotonia (Griggs et al., 1978). Recently, it has been reported that the drug may be able to shift the voltage dependence of wild-type hClC-1 channel activation toward more negative potentials, which might contribute to its antimyotonic effects (Eguchi et al., 2006). Because the G190S mutant induced a large positive shift of activation voltage dependence, we tested whether ACTZ is able to contrast G190S defect. The drug was tested at 10, 30, 100 and 300 μM on wild-type and G190S chloride currents in HEK293 cells (Fig. 7). The main effect of 100 μM ACTZ on WT channels consists in an ~50% increase of steady state currents at negative voltages (see arrows in Figs. 7A–C). The same effect was observed with 300 μM ACTZ on WT channels (not shown). In contrast, 300 μM ACTZ had little effect on G190S chloride currents, with variation in steady-state current amplitude minor than

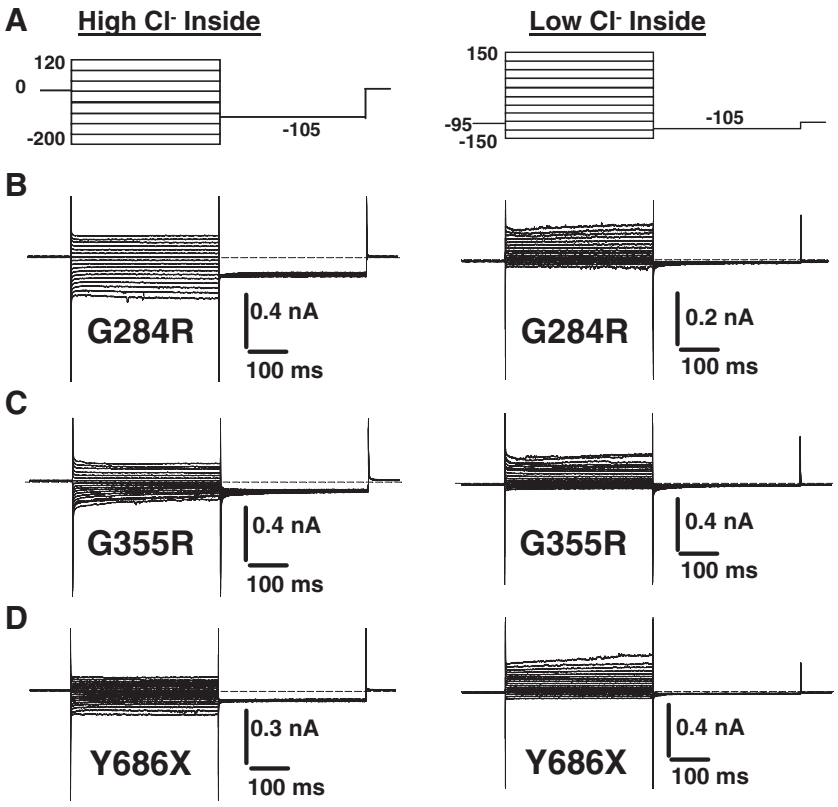

Fig. 4. Representative current traces elicited in HEK293 cells transfected with G284R, G355R, and Y686X myotonic hClC-1 mutants, using high and low intracellular chloride.

10% (Fig. 7D). The voltage-dependence of WT channel activation was negatively shifted by ~15 mV by ACTZ, whereas the voltage dependence of G190S remained quite unaffected by the drug (Figs. 7E, F). These experiments were performed using an internal solution containing 10 mM HEPES. Because it was proposed that ACTZ exerts its effects on ClC-1 through intracellular acidification, we also tested 100 μM ACTZ on WT and G190S chloride currents using only 1 mM HEPES in the pipette solution. In these conditions, the shift of channel activation voltage

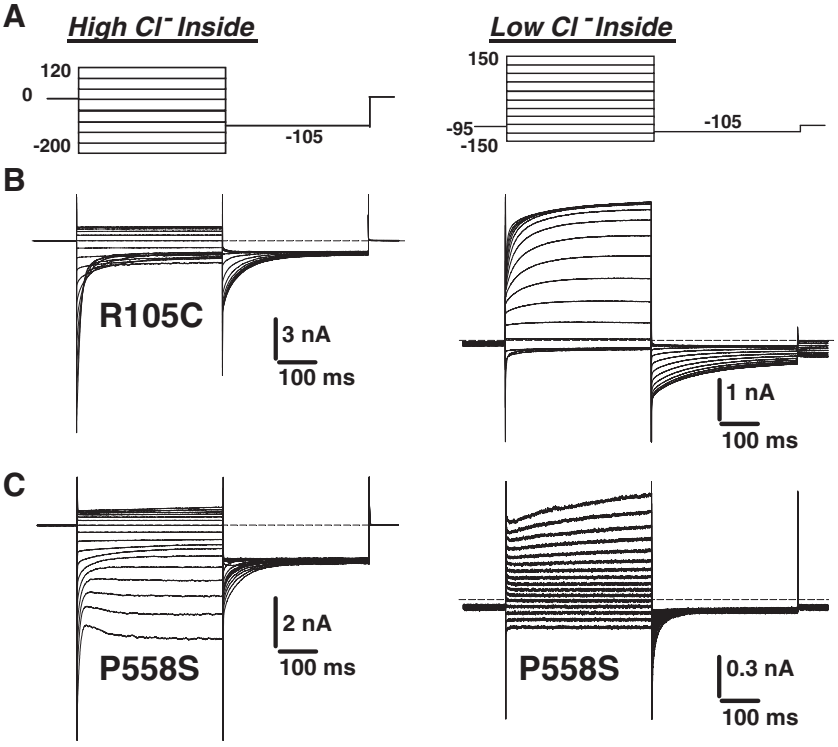

Fig. 5. Representative current traces elicited in HEK293 cells transfected with R105C and P558S myotonic hClC-1 mutants, using high and low intracellular chloride.

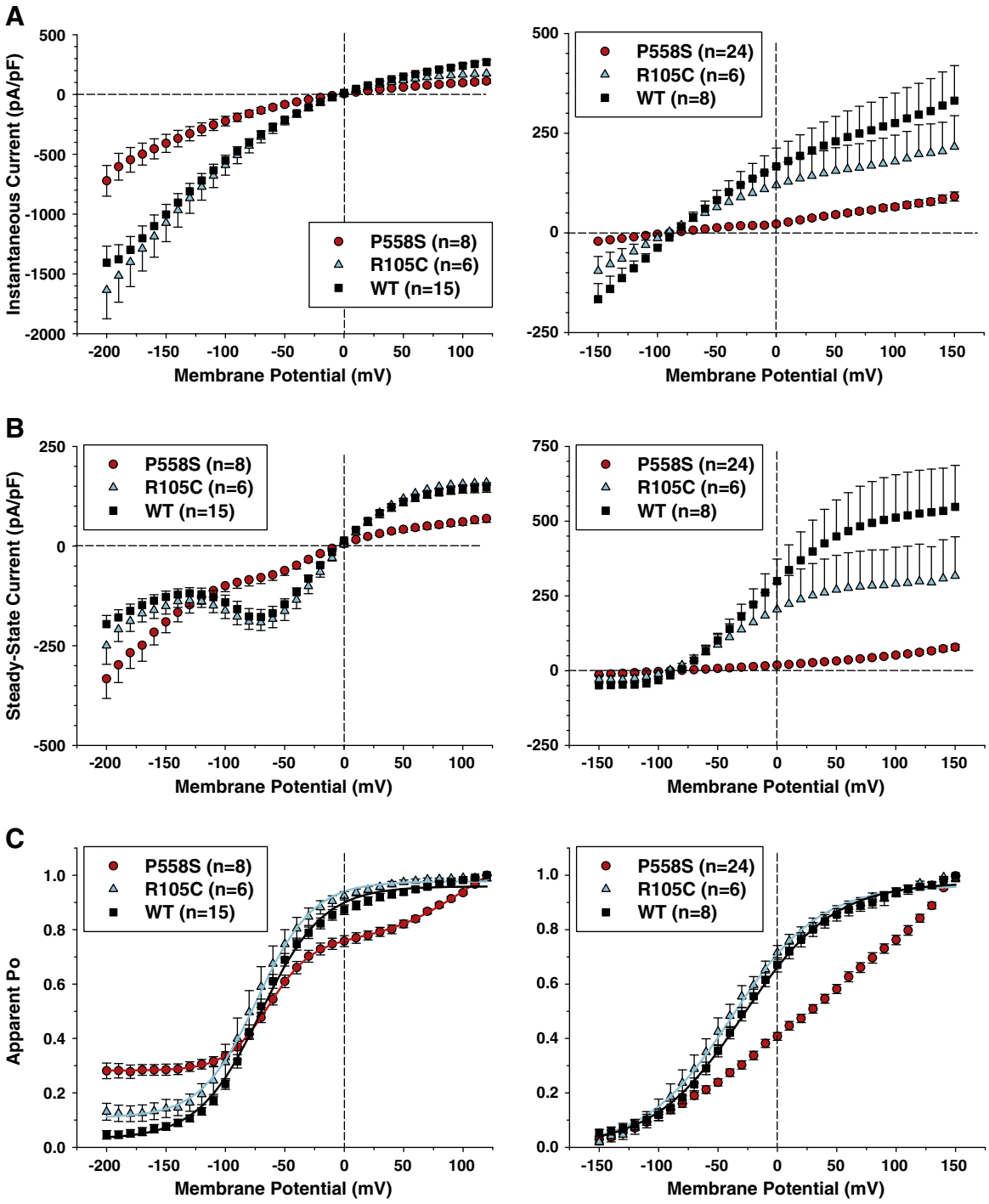

Fig. 6. Voltage-dependence of R105C and P558S myotonic hClC-1 channels in low intracellular chloride. A) The instantaneous current density–voltage relationships were obtained as in Fig. 1C, in high-chloride (left panel) and low-chloride (right panel) internal solutions. B) The steady-state current density–voltage relationships were drawn as in Fig. 1D, in high-chloride (left panel) and low-chloride (right panel) internal solutions. C) The voltage dependence of activation, determined as in Fig. 1D, were fit with a Boltzmann function (Eq. (1)). Fit parameters are reported in Table 1. The activation voltage dependences of R105C was very similar to WT. The relationship for P558S in high-chloride internal solution was best fit with a double Boltzmann function (Eq. (2)). No satisfactory fit was obtained for P558S in low intracellular chloride.

dependence was −20.6 ± 7.6 mV (n = 4) for WT and −3.3 ± 1.9 mV (n = 4) for G190S. This confirms the insensitivity of G190S to ACTZ.

Discussion

Although an overall reduction of sarcolemmal chloride currents is clearly responsible for the development of myotonia, little is known about the relation between the molecular alteration in ClC-1 channel function induced by each mutation and specific clinical features. In this study, we functionally characterize a large number of ClC-1 mutations in an attempt to complete our understanding of the genotype/phenotype relationship.

The G190S mutation induces a dramatic positive shift of activation voltage-dependence resulting in merely no detectable chloride currents within the physiological range. This confirms the results of a recently published study (Ulzi et al., 2012), but this shift was greatly accentuated in our hands. This may result in part from differences in data analysis, because we used currents measured at different voltages for normalization.

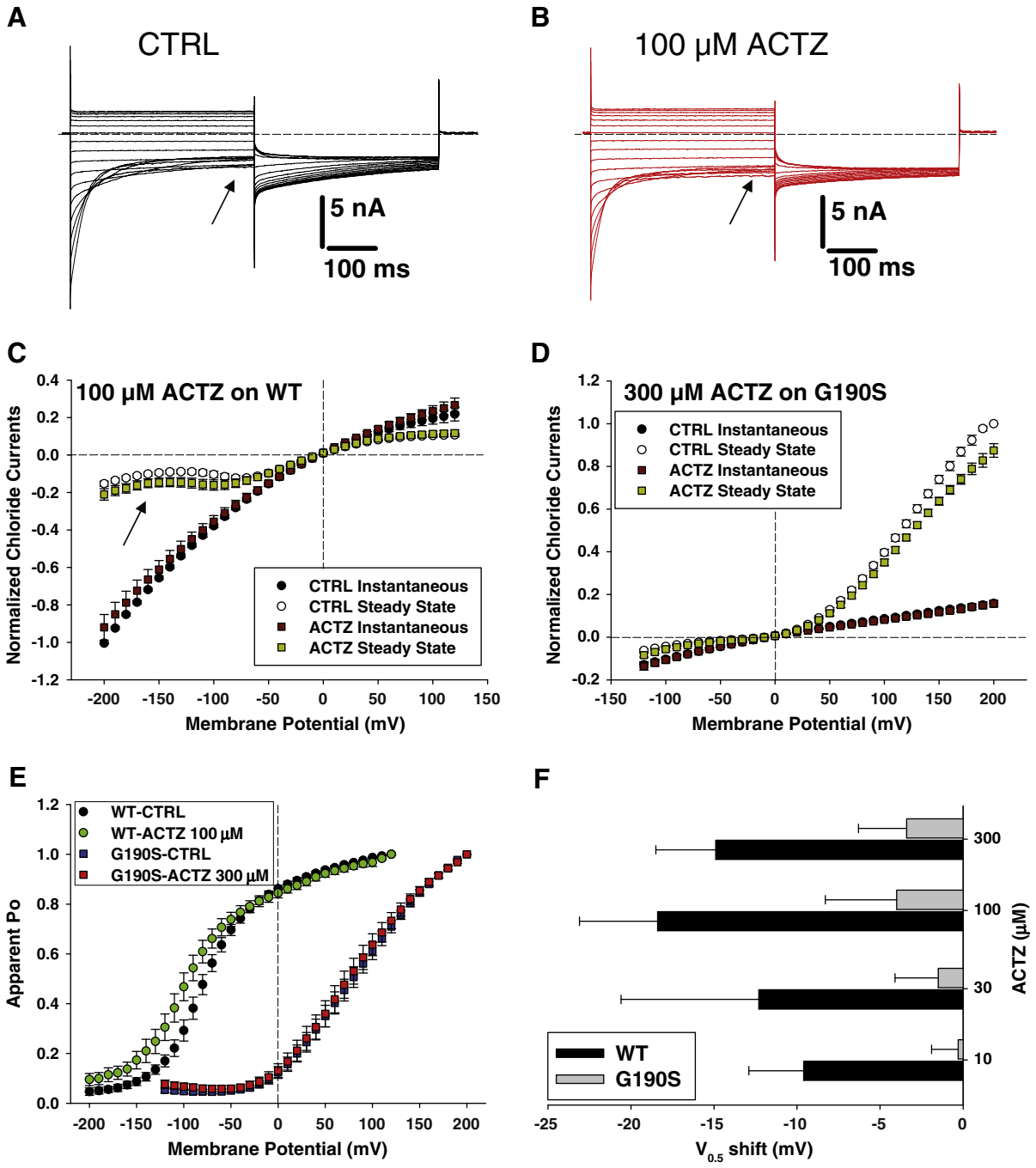

Fig. 7. Effects of acetazolamide (ACTZ) on wild-type (WT) and G190S hClC-1 chloride currents. Representative chloride currents are shown before (A) and after (B) application of 100 µM ACTZ to an HEK293 cell expressing WT hClC-1 channel. The internal chloride ion concentration was 134 mM. Cells were held at 0 mV and 400 ms voltage pulses were applied from −200 to +120 mV in 10-mV intervals every 3 s. For clarity only current traces obtained every 20 mV are shown. C) The current–voltage relationships were drawn for instantaneous and steady-state WT chloride currents, elicited before and after ACTZ application, and normalized with respect to instantaneous current recorded at −200 mV. Each point is the mean ± SEM from 7 cells. D) The chloride currents carried by G190S hClC-1 mutant were measured before and after application of 300 µM ACTZ to draw instantaneous and isochronal current–voltage relationships. Each point is the mean ± SEM from 6 cells. E) The voltage dependence of activation of WT (n = 7) and G190S (n = 6) channels was examined before and after application of 100 and 300 µM ACTZ, respectively. F) The half-maximum activation potential ($V_{0.5}$) of WT and G190S channels was determined before and after application of various ACTZ concentrations, by fitting the voltage dependence of activation with a Boltzmann function (Eq. (1)). The bar graph reports the shift of $V_{0.5}$ induced by ACTZ. Each bar is the mean ± SEM from 3-to-7 cells.

Such a voltage-dependent shift is common to different myotonic mutations (Pusch, 2002); the total lack of chloride currents within the physiological range of membrane voltages easily explains the hyper-excitability of myotonic muscles and the severity of myotonia generally observed in patients either homozygous for G190S or carrying G190S together with another mutation (Modoni et al., 2011; Shalata et al., 2010). Interestingly, three patients carrying the G190S mutation displayed a profound transitory depression of CMAP under neurophysiologic examination (Modoni et al., 2011), in accord with the proposed relationship between the shift of open probability curve and the CMAP decrement (Colding-Jorgensen, 2005).

The dramatic reduction of current densities with A531V is in accord with a previous study suggesting that the mutation may alter the trafficking of the channel toward the plasma membrane (Papponen et al., 2008). Nevertheless, our patch-clamp recordings, especially using high chloride internal solution, demonstrate that a number of functional mutant channels reach the plasma membrane and that the mutation does not modify channel gating. A recent study showing the

enhanced degradation of A531V confirms our observation (Lee et al., 2013). Because ion channel trafficking toward the membrane is notably dependent on a number of parameters, including temperature, calcium ion concentration and, more generally, cell metabolism, there is a possibility that membrane expression of A531V may endorse significant variations between individuals or physiological conditions, which would contribute to the reported variability in clinical manifestation and neurophysiologic transitory depression testing (Modoni et al., 2011; Sun et al., 2001). In addition, such a mechanism offers a possibility for developing pharmacological chaperones with therapeutic value. Such drugs would be able to increase the membrane expression of A531V channels, resulting in fully functional chloride currents.

The F167L mutation has been reported in various patient groups suffering from recessive myotonia congenita (George et al., 1994; Meyer-Kleine et al., 1995; Michel et al., 2007; Modoni et al., 2011; Ulzi et al., 2012). A previous patch-clamp examination using high-chloride internal concentration showed a small positive shift of Po voltage dependence, and slight alteration of deactivation kinetics (Zhang et al., 2000). In the current study, we found no significant difference with WT in chloride current density, voltage-dependence, and gating, either in high, intermediate, or low chloride ion concentration inside. Although F167 is not well conserved among CLC protein family members, most of the ClC channels display an aromatic residue at this position (tryptophan or tyrosine), except for ClC-7 that shows the non-aromatic leucine as the mutated ClC-1 in myotonic patients (Fig. 8). Nevertheless, F167L appears unlikely as a benign polymorphism in ClC-1, because it has never been found in ClC-1 of numerous control individuals. In addition, the contemporaneous occurrence of F167L in a DM2 patient was associated with unusual clinical findings, suggesting a pathogenic role for the ClC-1 channel mutation (Cardani et al., 2012).

In our previous and in the present study, F167L was found in association with seven different mutations in patients with recessive MC (Modoni et al., 2011). We thus studied the five exonic mutations associated with F167L, as none of these mutations have been previously functionally characterized. Among these, the G284R, G355R, and Y686X mutants did not generate any chloride currents in transfected HEK cells, suggesting a defect in protein synthesis or translocation to the membrane. Both G284 and G355 are well conserved residues among ClC proteins, located in the putative transmembrane S8 and S10 segments. Their substitution by a charged arginine residue dramatically abolished chloride currents. The Y686X mutation results in a truncated channel lacking the CBS2 domain and a major part of the CBS1–CBS2 linker in the C-terminal intracellular tail of the channel, which likely results in defective transport to the membrane (Estevez et al., 2004). The lack of chloride current with these mutants confirms their pathogenicity in producing myotonia. Despite such a drastic effect, patients carrying these mutations have a mild clinical phenotype and show a limited CMAP depression, suggesting that F167L, which behaves very similarly to WT, might temper the severity of symptoms. Indeed, homozygosity for G355R can produce a severe myotonic phenotype (Deymeer et al., 1998).

In symmetrical chloride, the P558S mutation introduced a singular slow activation of chloride currents at negative voltages, resulting in an increased Po at $V < -100$ mV. Such effect was not observed using the low chloride internal solution. Interestingly, a similar effect has been described for the nearby T550M mutation (Wu et al., 2002), suggesting that alteration of the putative intramembrane P segment, containing both T550 and P558, can profoundly affect the gating of ClC-1 channels. Nevertheless, this specific biophysical defect develops at very negative voltages and in high internal chloride only, and is unlikely involved in the pathogenicity of the mutant. Conversely, another effect of P558S consists in the drastic reduction of chloride current densities at physiological membrane voltages, which is likely responsible for muscle hyperexcitability. In this specific context, the F167L mutation does not mitigate the clinical phenotype, which is characterized by severe generalized myotonia and muscle stiffness; whether P558S may exert a dominant negative effect on F167L would require further investigation. Another possibility may be the expression of disease modifiers in the P558S/F167L carrier.

The mutation R105C was first identified in a German patient and then in a patient from Southern Italy, both suffering from recessive myotonia (Meyer-Kleine et al., 1995; Modoni et al., 2011). A charged amino acid residue (arginine or lysine) is present at this position in 5 members of the CLC protein family but absent from 4 others (Fig. 8). We show here that the substitution of cysteine for arginine has little effect on ClC-1 gating. The unique effect is a small and nonsignificant reduction of current density compared to wild-type in low internal chloride condition. Thus the pathogenic mechanism of R105C remains elusive as for F167L. Interestingly, the Italian patient carrying R105C shows the most severe clinical phenotype among F167L-carrying patients, including significant transitory CMAP depression under neurophysiological test, lower limbs hypertrophy, and occasional need of the antimyotonic drug mexiletine (200 mg a day), thereby suggesting unrevealed pathogenic mechanisms of these mutations or the presence of disease modifiers (Modoni et al., 2011).

Acetazolamide has been used empirically for its beneficial action on a variety of disorders of skeletal muscle membrane excitability including

channel	position	Amino acids																
CLC-1	F167	L	Q	F	L	V	W	V	T	F	P	L	V	L	I	L	F	S	A
CLC-2	Y140	L	Q	Y	L	A	W	V	T	Y	P	V	V	L	I	T	F	S	A
CLC-KA	Y99	L	R	Y	L	S	W	T	V	Y	P	V	A	L	V	S	F	S	S
CLC-KB	Y99	L	R	Y	L	S	W	T	V	Y	P	V	A	L	V	S	F	S	S
CLC-4	W159	L	N	Y	L	M	Y	I	L	W	A	L	L	F	A	F	L	A	V
CLC-5	W216	V	N	Y	F	M	Y	V	L	W	A	L	L	F	A	F	L	A	V
CLC-3	W217	M	N	Y	I	M	Y	I	F	W	A	L	S	F	A	F	L	A	V
CLC-6	F135	L	S	L	L	E	L	L	G	F	N	L	T	F	V	F	L	A	S
CLC-7	L182	F	S	L	L	L	W	A	T	L	N	A	A	F	V	L	V	G	S

channel	position	Amino acids																	
CLC-1	R105	S	K	C	Q	D	C	I	H	R	L	G	Q	V	V	R	R	K	L
CLC-2	R78	A	R	C	R	V	C	S	V	R	C	H	K	F	L	V	S	R	V
CLC-KA	E37	R	R	A	I	Q	G	G	L	E	W	L	K	Q	K	V	F	R	L
CLC-KB	E37	R	R	G	I	R	G	G	L	E	W	L	K	Q	K	L	F	R	L
CLC-4	K52	D	R	H	R	K	I	T	S	K	S	K	E	S	I	W	E	F	I
CLC-5	K109	D	R	H	R	E	I	T	N	K	S	K	E	S	T	W	A	L	I
CLC-3	K110	E	R	H	R	R	I	N	S	K	K	K	E	S	A	W	E	M	T
CLC-6	L62	D	R	C	I	N	D	P	Y	L	E	V	L	E	T	M	D	N	K
CLC-7	L108	D	N	S	E	N	Q	L	F	L	E	E	E	R	R	I	N	H	T

Fig. 8. Multiple amino acid sequence alignments of human ClC proteins with Clustal 2.1.

sodium and chloride channel myotonias, paramyotonia, hyper- and hypokalemic periodic paralysis, and Andersen's syndrome (Griggs et al., 1978; Ruff, 2006). One possible mechanism accounting for membrane electrical stabilization by ACTZ likely consists in the opening of calcium-activated potassium channels (Tricarico et al., 2000). More recently, it was proposed that the drug is also able to shift ClC-1 open probability toward more negative voltage, resulting in an increased chloride current and consequent membrane voltage stabilization (Eguchi et al., 2006). Because G190S induced a great positive shift of ClC-1 open probability, we wondered whether ACTZ may be able to counteract the effect of the mutation. Although we were able to confirm activating effects of ACTZ on WT channels, no significant effect was observed on G190S chloride currents, suggesting that the mutation hampers channel sensitivity to the drug and possibly to intracellular pH.

In conclusion, the functional characterization of a large spectrum of recessive ClC-1 mutations underscores a variety of molecular mechanisms, all leading to a reduction of chloride currents likely responsible for the clinical phenotype. Our study suggests that these mechanisms may however influence the clinical phenotype. For instance, it appears that the great shift of channel activation toward positive voltages, as for G190S, is a likely promoter of transitory depression and weakness. Such a knowledge is of fundamental importance for the development of selective drugs able to correct specifically the biophysical defect and to exert efficient and safe antimyotonia therapy. Selective ligands for ClC-1 channels are dramatically lacking, although recent progress have been reported in identifying potent inhibitors of various ClC proteins (Liantonio et al., 2008; Matulef et al., 2008). Although acetazolamide increases wild-type chloride currents in vitro, ClC-1 mutations can impair such effect and may limit its clinical efficiency, especially in recessive carriers. Further studies are warranted to complete our understanding of the genotype–phenotype relationship in chloride channel myotonia and to identify promising antimyotonia therapeutics.

Conflict of interest

All authors claim no conflict of interest.

Acknowledgments

This study was supported by grants from the Italian “Comitato Telethon Fondazione Onlus” (Not-for-Profit; grant number GGP10101) and the French “Association Française contre les Myopathies” (Not-for-Profit; grant number #15020). The Italian association M.i.A. onlus (“Miotonici in Associazione”) is acknowledged for dedicated collaboration.

References

Aminoff, M.J., Layzer, R.B., Satya-Murti, S., Faden, A.I., 1977. The declining electrical response of muscle to repetitive nerve stimulation in myotonia. Neurology 27, 812–816.
Cardani, R., Giagnacovo, M., Botta, A., Rinaldi, F., Morgante, A., Udd, B., Raheem, O., Penttila, S., Suominen, T., Renna, L.V., Sansone, V., Bugiardini, E., Novelli, G., Meola, G., 2012. Co-segregation of DM2 with a recessive CLCN1 mutation in juvenile onset of myotonic dystrophy type 2. J. Neurol. 259, 2090–2099.
Colding-Jorgensen, E., 2005. Phenotypic variability in myotonia congenita. Muscle Nerve 32, 19–34.
Desaphy, J.-F., De Luca, A., Tortorella, P., De Vito, D., George Jr., A.L., Conte Camerino, D., 2001. Gating of myotonic Na channel mutants defines the response to mexiletine and a potent derivative. Neurology 57, 1849–1857.
Desaphy, J.-F., De Luca, A., Didonna, M.P., George Jr., A.L., Conte Camerino, D., 2004. Different flecainide sensitivity of hNav1.4 channels and myotonic mutants explained by state-dependent block. J. Physiol. 554 (2), 321–334.
Desaphy, J.-F., Modoni, A., LoMonaco, M., Conte Camerino, D., 2013. Dramatic improvement of myotonia permanens with flecainide: a two-case report of a possible bench-to-bedside pharmacogenetics strategy. Eur. J. Clin. Pharmacol. 69, 1037–1039.
Deymeer, F., Cakirkaya, S., Serdaroğlu, P., Schleithoff, L., Lehmann-Horn, F., Rüdel, R., Ozdemir, C., 1998. Transient weakness and compound muscle action potential decrement in myotonia congenita. Muscle Nerve 21 (10), 1334–1337.
Eguchi, H., Tsujino, A., Kaibara, M., Hayashi, H., Shirabe, S., Taniyama, K., Eguchi, K., 2006. Acetazolamide acts directly on the human skeletal muscle chloride channel. Muscle Nerve 34, 292–297.
Estevez, R., Pusch, M., Ferrer-Costa, C., Orozco, M., Jentsch, T.J., 2004. Functional and structural conservation of CBS domains from CLC chloride channels. J. Physiol. 557, 363–378.
George Jr., A.L., Crackower, M.A., Abdalla, J.A., Hudson, A.J., Ebers, G.C., 1993. Molecular basis of Thomsen's disease (autosomal dominant myotonia congenita). Nat. Genet. 3 (4), 305–310.
George Jr., A.L., Sloan-Brown, K., Fenichel, G.M., Mitchell, G.A., Spiegel, R., Pascuzzi, R.M., 1994. Nonsense and missense mutations of the muscle chloride channel gene in patients with myotonia congenita. Hum. Mol. Genet. 3, 2071–2072.
Griggs, R.C., Moxley III, R.T., Riggs, J.E., Engel, W.K., 1978. Effects of acetazolamide on myotonia. Ann. Neurol. 3, 531–537.
Koch, M.C., Steinmeyer, K., Lorenz, C., Ricker, K., Wolf, F., Otto, M., et al., 1992. The skeletal muscle chloride channel in dominant and recessive human myotonia. Science 257, 797–800.
Lee, T.T., Zhang, X.D., Chuang, C.C., Chen, J.J., Chen, Y.A., Chen, S.C., Chen, T.Y., Tang, C.Y., 2013. Myotonia congenita mutation enhances the degradation of human CLC-1 chloride channels. PLoS One 8 (2), e55930.
Liantonio, A., Picollo, A., Carbonara, G., Fracchiolla, G., Tortorella, P., Loiodice, F., Laghezza, A., Babini, E., Zifarelli, G., Pusch, M., Conte Camerino, D., 2008. Molecular switch for CLC-K Cl-channel block/activation: optimal pharmacophoric requirements towards high-affinity ligands. Proc. Natl. Acad. Sci. U. S. A. 105 (4), 1369–1373.
Matulef, K., Howery, A.E., Tan, L., Kobertz, W.R., Du Bois, J., Maduke, M., 2008. Discovery of potent ClC chloride channel inhibitors. ACS Chem. Biol. 3, 419–428.
Meyer-Kleine, C., Steinmeyer, K., Ricker, K., Jentsch, T.J., Koch, M.C., 1995. Spectrum of mutations in the major human skeletal muscle chloride channel gene (CLCN1) leading to myotonia. Am. J. Hum. Genet. 57, 1325–1334.
Michel, P., Sternberg, D., Jeannet, P.-Y., Dunand, M., Thonney, F., Kress, W., Fontaine, B., Fournier, E., Kuntzer, T., 2007. Comparative efficacy of repetitive nerve stimulation, exercise, and cold in differentiating myotonic disorders. Muscle Nerve 36, 643–650.
Modoni, A., D'Amico, A., Dallapiccola, B., Mereu, M.L., Merlini, L., Pagliarani, S., Pisaneschi, E., Silvestri, G., Torrente, I., Valente, E.M., Lo Monaco, M., 2011. Low-rate repetitive nerve stimulation protocol in an Italian cohort of patients affected by recessive myotonia congenita. J. Clin. Neurophysiol. 28, 39–44.
Papponen, H., Nissinen, M., Kaisto, T., Myllyla, V.V., Myllila, R., Metsikko, K., 2008. F413C and A531V but not R894X myotonia congenita mutations cause defective endoplasmic reticulum export of the muscle-specific chloride channel ClC-1. Muscle Nerve 37, 317–325.
Pusch, M., 2002. Myotonia caused by mutations in the muscle chloride channel gene CLCN1. Hum. Mutat. 19, 423–434.
Ruff, R.L., 2006. Sour on the inside, calm on the outside: how acetazolamide may stabilize membrane excitability. Muscle Nerve 34, 263–264.
Saviane, C., Conti, F., Pusch, M., 1999. The muscle chloride channel ClC-1 has a double-barreled appearance that is differentially affected in dominant and recessive myotonia. J. Gen. Physiol. 113 (3), 457–468.
Shalata, A., Furman, H., Adir, V., Adir, N., Hujeirat, Y., Shalev, S.A., Borochowitz, Z.U., 2010. Myotonia congenita in a large consanguineous Arab family: insight into the clinical spectrum of carriers and double heterozygotes of a novel mutation in the chloride channel CLCN1 gene. Muscle Nerve 41, 464–469.
Statland, J.M., Bundy, B.N., Wang, Y., Rayan, D.R., Trivedi, J.R., Sansone, V.A., Salajegheh, M.K., Venance, S.L., Ciafaloni, E., Matthews, E., Meola, G., Herbelin, L., Griggs, R.C., Barohn, R.J., Hanna, M.G., Consortium for Clinical Investigation of Neurologic Channelopathies, 2012. Mexiletine for symptoms and signs of myotonia in nondystrophic myotonia: a randomized controlled trial. JAMA 308 (13), 1357–1365.
Sun, C., Tranebjærg, L., Torbergsen, L., Holmgren, G., Van Ghelue, M., 2001. Spectrum of CLCN1 mutations in patients with myotonia congenita in Northern Scandinavia. Eur. J. Hum. Genet. 9, 903–909.
Tricarico, D., Barbieri, M., Conte Camerino, D., 2000. Acetazolamide opens the muscular KCa2 + channel: a novel mechanism of action that may explain the therapeutic effect of the drug in hypokalemic periodic paralysis. Ann. Neurol. 48 (3), 304–312.
Trip, J., Drost, G., Ginjaar, H.B., Nieman, F.H., van der Kooi, A.J., de Visser, M., van Engelen, B.G., Faber, C.G., 2009. Redefining the clinical phenotypes of non-dystrophic myotonic syndromes. J. Neurol. Neurosurg. Psychiatry 80 (6), 647–652.
Ulzi, G., Lecchi, M., Sansone, V., Redaelli, E., Corti, E., Saccomanno, D., Pagliarani, S., Corti, S., Magri, F., Raimondi, M., D'Angelo, G., Modoni, A., Bresolin, N., Meola, G., Wanke, E., Comi, G.P., Lucchiari, S., 2012. Myotonia congenita: novel mutations in CLCN1 gene and functional characterizations in Italian patients. J. Neurol. Sci. 318 (1–2), 65–71.
Wu, F.-F., Ryan, A., Devaney, J., Warnstedt, M., Korade-Mirnics, Z., Poser, B., Escriva, M.J., Pegoraro, E., Yee, A.S., Felice, K.J., Giuliani, M.J., Mayer, R.F., Mongini, T., Palmucci, L., Marino, M., Rudel, R., Hoffman, E.P., Fahlke, C., 2002. Novel CLCN1 mutations with unique clinical and electrophysiological consequences. Brain 125, 2392–2407.
Zhang, J., Bendahhou, S., Sanguinetti, M.C., Ptacek, L.J., 2000. Functional consequences of chloride channel gene (CLCN1) mutations causing myotonia congenita. Neurology 54, 937–942.